Identification of the Catalytic Mg^{2+} Ion in the Hepatitis Delta Virus Ribozyme

SUPPORTING INFORMATION

Ji Chen[‡], Abir Ganguly[‖,a], Zulaika Miswan[‡], Sharon Hammes-Schiffer[‖,a], Philip C. Bevilacqua[‖,§,*], [‡]Barbara L. Golden[‡,*]

[‡]Department of Biochemistry, Purdue University, 175 South University Street, West Lafayette, Indiana 47907. [‖]Department of Chemistry and [§]Center for RNA Molecular Biology, The Pennsylvania State University, University Park, Pennsylvania 16802. [a]Present address: Department of Chemistry, University of Illinois at Urbana-Champaign, Urbana, Illinois 61801.

[†] This project was supported by NIH grant R01GM095923 (B.L.G and P.C.B), NIH grant GM56207 (S.H.S.), instrumentation funded by the NSF through grant OCI-0821527, the Purdue University Department of Biochemistry, the Markey Center for Structural Biology and the Purdue University Center for Cancer Research (B.L.G.).

*To whom correspondence should be addressed. B.L.G.: telephone (765) 496-6165; fax (765) 494-7897; email: barbgolden@purdue.edu. P.C.B. telephone (814) 863-3812; fax (814) 865-2927. e-mail: pcb5@psu.edu.

Contents:

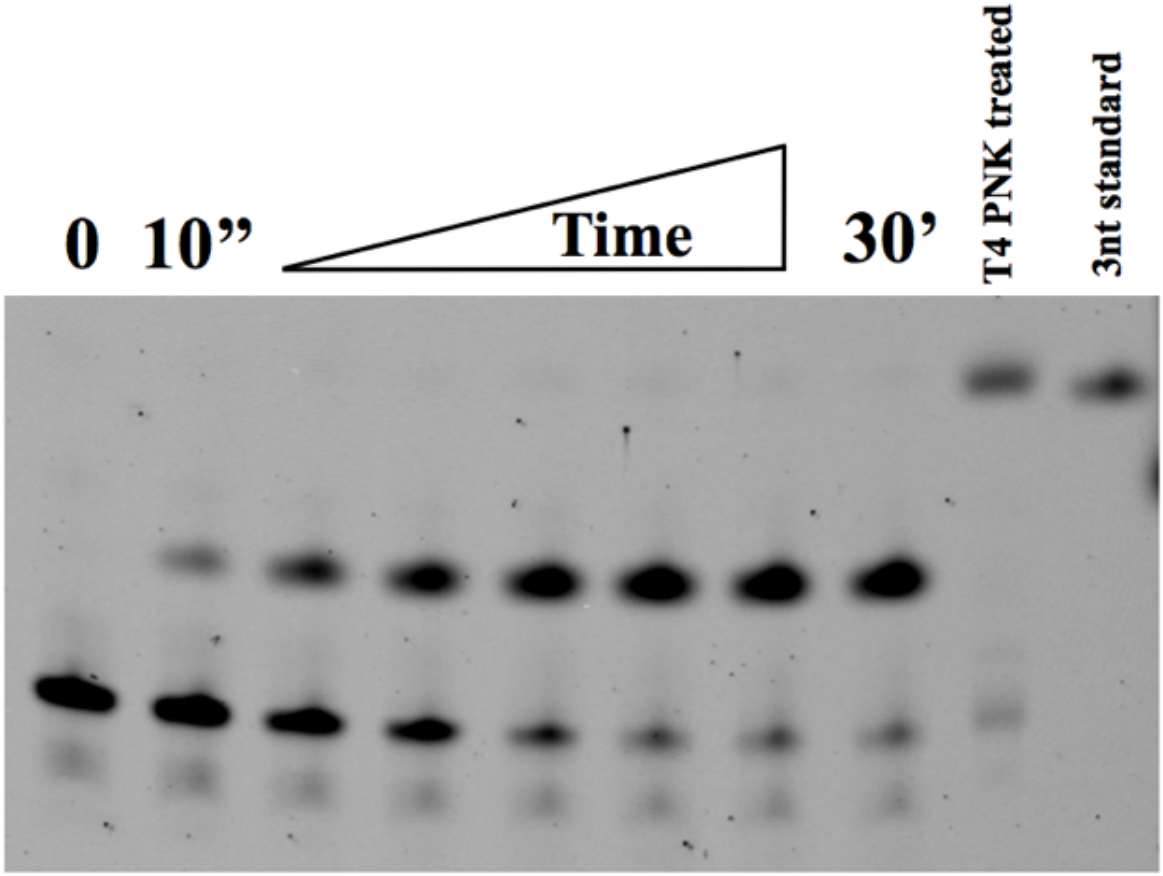

Figure S1. Identification of the HDV ribozyme cleavage product. The WT HDV ribozyme was mixed with a fluorophore-labeled substrate DY547-UAU*GGCUUGCA and 0.5 mM $MgCl_2$ in MOPS pH 7.0. Ribozyme cleavage resulted in a product with reduced mobility as predicted for the reaction product, DY547-UAU with a 2’, 3’-cyclic phosphate terminus, as the fluorophore is bulky and carries a positive charge. To verify the nature of this product, it was treated with T4 polynucleotide kinase and calf intestinal phosphatase to remove the 2’,3’-cyclic phosphate[(1)] and generate DY547-UAU with free 2’- and 3’-hydroxyl groups. This product co-migrates with an authentic DY547-UAU standard (see last two right-hand lanes).

Materials and Methods for Figure S2

pH-rate profile of the G25A•U20C double mutant in the absence of Mg2+. To characterize the pH dependence of ribozyme reaction under Mg^{2+}-free conditions, the *cis*-cleaving one-piece -30/99 HDV ribozyme was transcribed as described above for the *trans*-cleaving ribozyme. This RNA is based on the sequence of the genomic HDV ribozyme and incorporates the G11C mutation that enhances the folding properties of the RNA.[(2)] It has a 5'-end that is 30 nucleotides upstream of the cleavage site and a 3'-end that is 99 nucleotides downstream of the cleavage site. This is referred to as the wild-type ribozyme for the purpose of this study. The A25•C20 mutation was introduced into this construct to generate an G25A•U20C double mutant self-cleaving RNA. Preparation of the one-piece RNA was necessary because the two-piece HDV ribozyme does not react in the conditions needed to monitor the reaction in the absence of Mg^{2+} ion.

The 5'-end of the RNA was radiolabeled using polynucleotide kinase and [γ-^{32}P]-ATP and gel-purified as described for the two-piece ribozyme. To perform the cleavage assays, ~2 nM of labeled HDV ribozyme was renatured at 55°C for 10 min in TE buffer (0.5 mM Tris-HCl pH7.5 and 0.05 mM EDTA pH 8.0) and allowed to cool down at room temperature for 10 min. The folded RNA was then pre-incubated at 37°C for 2 min with saturating 10 μM DNA oligomer (AS1) that is complementary to the single-stranded RNA upstream of the cleavage site (nucleotides -30 through -3) in 50 mM (final concentration) of one of the following buffers: potassium acetate (pH5.0 and 5.5), potassium MES (pH6.0 and pH6.5) or Tris-HCl (pH7.0-pH8.5). AS1 DNA oligomer sequesters the inhibitory strand upstream of the cleavage site and helps to prevent misfolding.[(2)] All the buffers were supplemented with 100 mM EDTA (final concentration) prior to adjusting the pH to the final values. No attempt was made to correct the meter reading for effects on ionic strength. This may lead to an underestimate of pK_a values by ~ 0.5 units, but does not affect comparative values.[(3)] A zero time point was removed followed by adding pre-warmed 1M NaCl to initiate the reaction. The time course experiment was incubated at 37°C for up to ~200 h. Samples at appropriate time points were removed, quenched and analyzed on a 6% denaturing PAGE. Quantitation was performed by a PhosphorImager (Molecular Dynamics). Reaction progress was analyzed by KaleidaGraph 4.1 (Synergy Software). Data fitting was described in Materials and Methods, with an exception of the G25A•U20C double mutant reacting at pH8.0, where $f = k_{obs}t$ was used to determine the k_{obs} value (~60% of completion was reached at 144h, only the initial ~30% was used for data fitting).

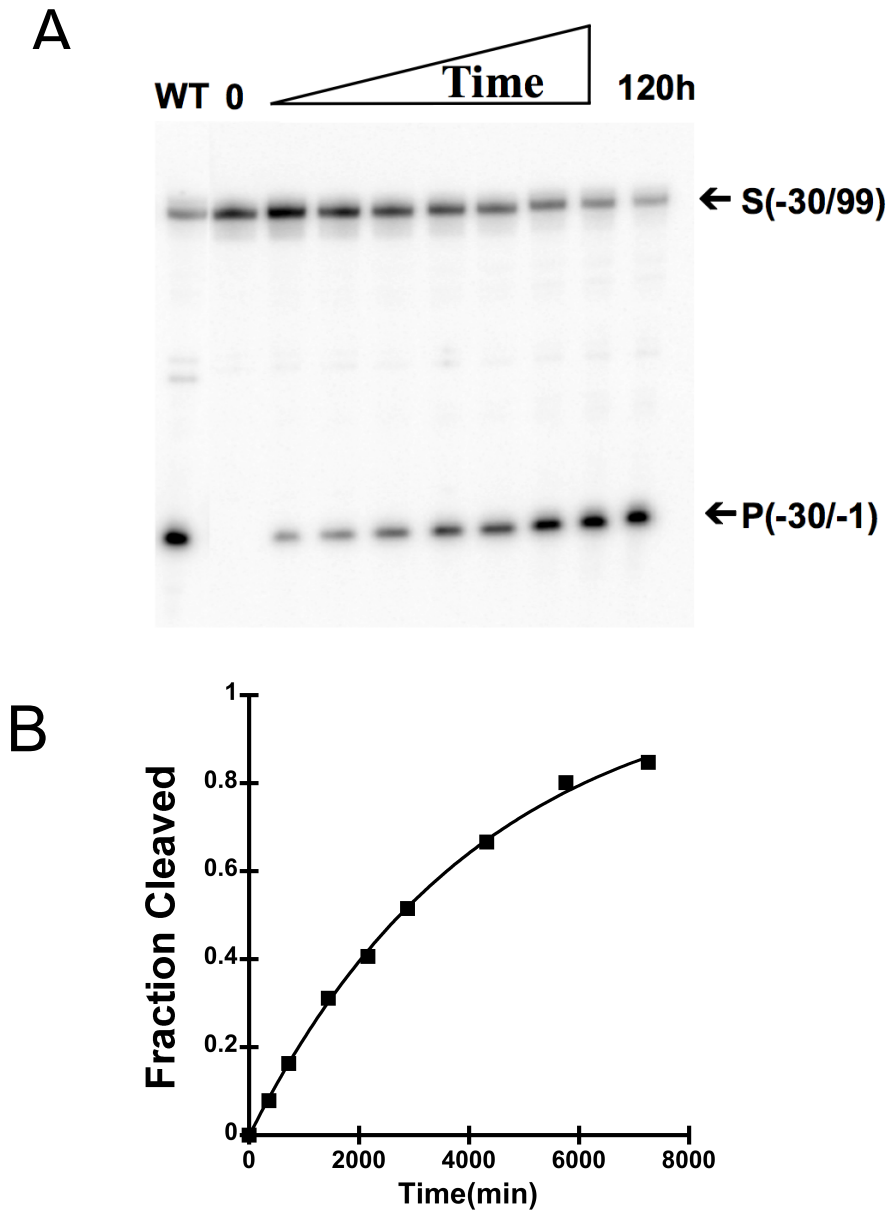

Figure S2. The self-cleavage reaction of the G25A•U20C double mutant. **A.** The denaturing PAGE shows a cleavage reaction of the 5'-end-labeled G25A•U20C double mutant in 1M NaCl, 50 mM Tris and 100 mM EDTA at pH 7.0. The -30/99 precursor ribozyme starting material and the -30/-1 cleavage product are indicated as S and P, respectively. A wild type ribozyme (WT) cleavage reaction at 24 h under the same conditions is shown for comparison. **B.** Panel A was quantitated and fraction of cleavage was plotted against time to yield the graph of reaction progress. The G25A•U20C double mutant cleaves to more than 80% completion at 120 h in a monophasic fashion. The data were fit to equation (1).

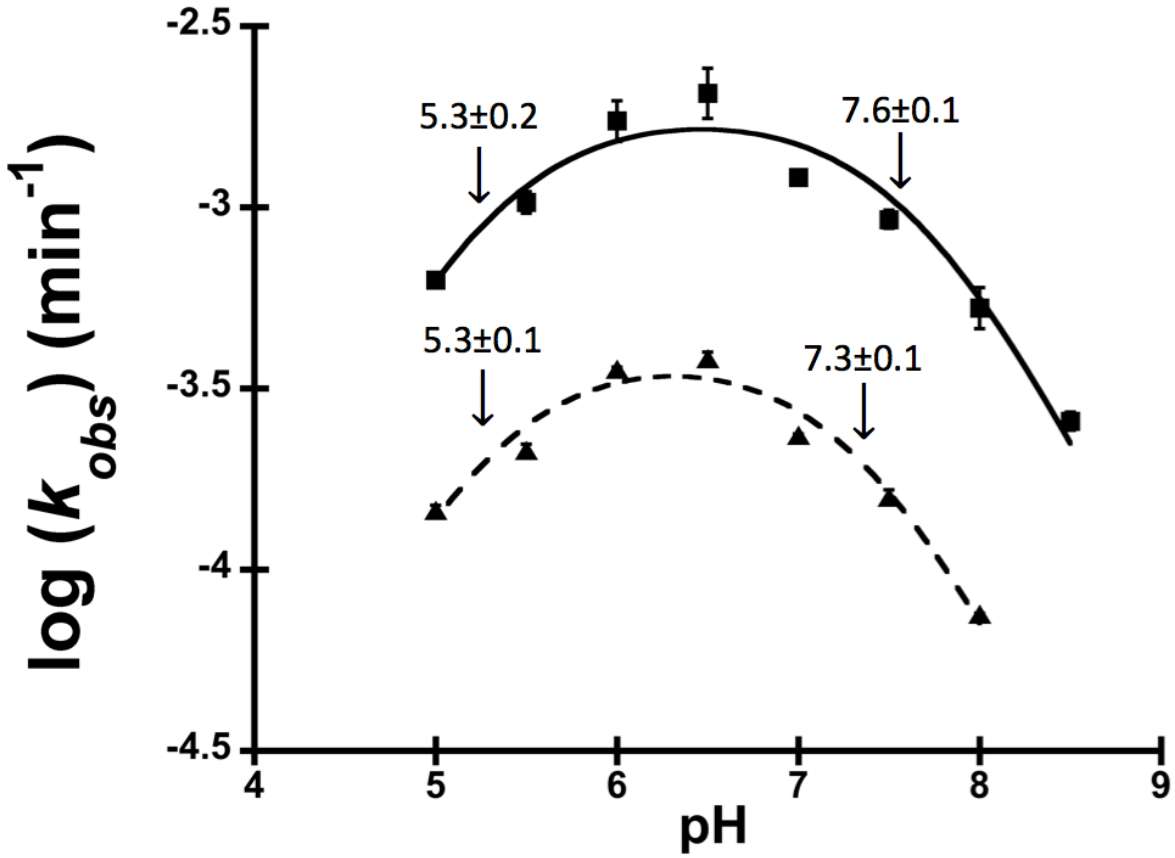

Figure S3. The pH-rate profiles for the self-cleavage reactions of the G25A•U20C double mutant and WT in the absence of Mg^{2+} ion. The reactions were performed in 1 M NaCl, 50 mM buffer and 100 mM EDTA for the WT (squares) and the G25A•U20C double mutant (triangles). The data were fit to equation (5) to account for the two ionizable groups (See Discussion), which yielded apparent pK_a's of 5.3 ± 0.2 and 7.6 ± 0.1 for the WT and apparent pK_a's of 5.3 ± 0.1 and 7.3 ± 0.1 for the the G25A•U20C double mutant, as illustrated in the figure.

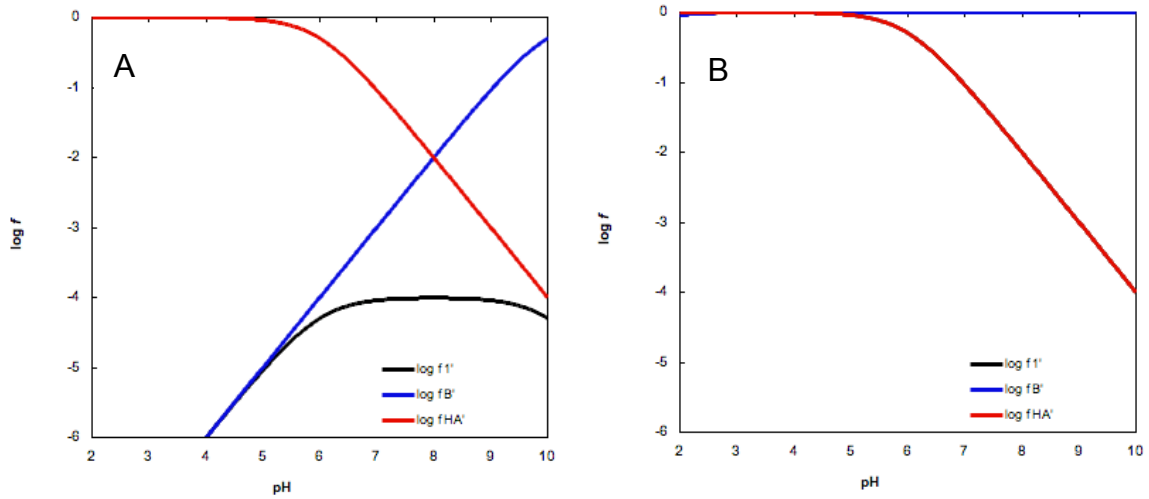

Figure S4. Sum of rate-pH profiles to generate observed rate-pH profiles. Simulations are according to Bevilacqua.[4] **A.** Origin of rate-pH profile in the *presence* of catalytic Mg^{2+}. The functional form of the base—either magnesium hydroxide as a Brønsted (general) base or magnesium as a Lewis acid and OH- as a specific base (see Figure S5A and B for these and related, dual mechanisms)—is depicted in blue, and the functional form of the acid, presumably $C75^{+}$, is depicted in red. Their logarithmic sum, which represents the fraction of the ribozyme in the fully functional form, is shown in black. The shape of the black curve is similar to the rate-pH profiles seen for WT in the presence of Mg^{2+} (Figure 4, squares). **B.** Origin of rate-pH profile in the *absence* of catalytic Mg^{2+}. The functional form of the base—either water or a non-ionizing functional group on the RNA, and/or some other base possibly in a non-rate limiting step (see Figure S5C)—is depicted in blue, and the functional form of the acid, presumably $C75^{+}$, is depicted in red. Their logarithmic sum, which represents the fraction of the ribozyme in the fully functional form, is black (hidden under red curve). The shape of the black curve is similar to profiles seen for the G25A•U20C double mutant in the presence of Mg^{2+}, which does not participate in the reaction (Figure 4, triangles). In both simulations (panels A and B), the pK_a of the general acid is set at 6; the pK_a of the general base is set at 10 in panel A and at -1.7 (the pK_a of water) in panel B. Experiments can only be conducted up to pH~8 owing to alkaline denaturation of the ribozyme, which comes from hydroxide competing for hydrogen bonding.[5] Another simulation could be made for panel B with a pK_a of 5.4 for the general base that would produce the slight low pH arm in Figure 4 (triangles); this was not done here because of the possibility that this effect arises from acid denaturation or contribution of a catalytic metal ion only at low pH (see main text).

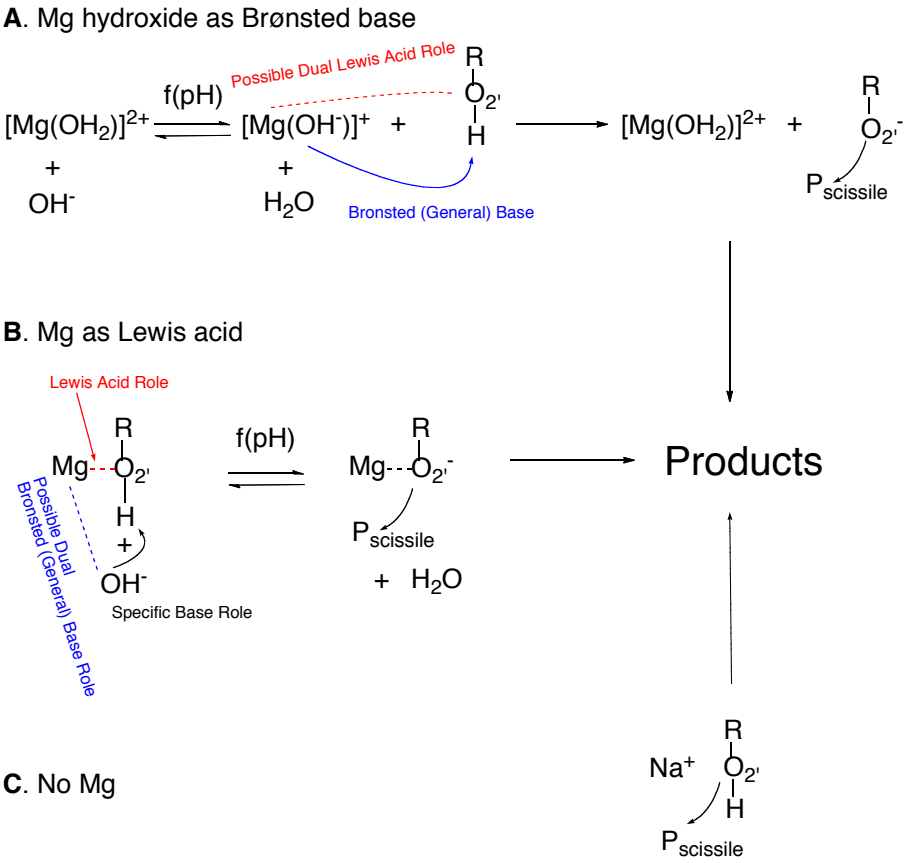

Figure S5. Possible mechanisms for deprotonation of the 2'-hydroxyl. Panels **A** and **B** depict mechanisms in the *presence* of Mg^{2+}, which are for WT, while panel **C** depicts a mechanism in the *absence* of Mg^{2+}, which is for G25A•U20C double mutant. Steps that are a function of pH, which is important in interpreting rate-pH profiles such as in Figure S4, are noted. **A.** Magnesium hydroxide serves as a Brønsted (general) base (blue), with a possible dual role as a Lewis acid at the 2'O (red). **B.** Magnesium serves as a Lewis acid (red), with a possible dual role as a general base through a Mg^{2+}-bound hydroxide (blue), otherwise some other species needs to act as the base in a pH-dependent fashion, such as hydroxide as a specific base. Alternately, the pK_a reflects the pK_a of the 2'OH of U(-1) itself. **C.** Reaction without catalytic magnesium. Here population of the general base is independent of pH (Figure S4B, blue line), so either water (pK_a of -1.7) or some other low pK_a group (pK_a should be <~4, the lower end of the experimental pH range) perhaps on the RNA (not shown) acts as the base, and/or proton transfer from the 2'OH occurs in a non rate-determining step. Na^+ bound nearby could have a general electrostatic effect (see text). See Emilsson *et al.* for related mechanisms.[6] A reason hydroxide could deprotonate the 2'OH in panel B but not C is that the Mg^{2+} could lower the pK_a of the 2'OH in panel B.

Table S1. Statistics from MD simulation of the G25A•U20C double mutant of the HDV ribozyme[a]

Trajectory	Mg^{2+} ion present initially	A25(N1)-C20(N4) (Å)	A25(N6)-C20(N3) (Å)	A25(N6)-metal ion (Å)	A25(N7)-metal ion (Å)	C20(O2)-metal ion (Å)
1	Yes	3.10 (0.19)	2.91 (0.09)	4.32 (0.23)	4.76 (0.17)	4.26 (0.22)
2	Yes	3.00 (0.12)	2.90 (0.09)	4.25 (0.17)	4.90 (0.20)	4.00 (0.16)
1	No	3.03 (0.15)	2.97 (0.16)	3.41 (0.35)	5.20 (0.29)	2.53 (0.53)
2[b]	No	3.05 (0.15)	2.97 (0.12)	4.23 (0.32)	4.95 (0.26)	4.14 (0.66)

[a]Values are distances with standard deviations shown in parentheses.

[b]In this trajectory, a sodium ion did not move into the catalytic site until the first 1.5 ns. The data shown here was collected after the sodium ion moved in, over the next 23.5 ns.

References

1. Morse, D. P., and Bass, B. L. (1997) Detection of inosine in messenger RNA by inosine-specific cleavage, *Biochemistry 36*, 8429-8434.
2. Chadalavada, D. M., Knudsen, S. M., Nakano, S., and Bevilacqua, P. C. (2000) A role for upstream RNA structure in facilitating the catalytic fold of the genomic hepatitis delta virus ribozyme, *J. Mol. Biol. 301*, 349-367.
3. Cerrone-Szakal, A. L., Siegfried, N. A., and Bevilacqua, P. C. (2008) Mechanistic characterization of the HDV genomic ribozyme: solvent isotope effects and proton inventories in the absence of divalent metal ions support C75 as the general acid, *J. Amer. Chem. Soc. 130*, 14504-14520.
4. Bevilacqua, P. C. (2003) Mechanistic considerations for general acid-base catalysis by RNA: revisiting the mechanism of the hairpin ribozyme, *Biochemistry 42*, 2259-2265.
5. Moody, E. M., Lecomte, J. T., and Bevilacqua, P. C. (2005) Linkage between proton binding and folding in RNA: a thermodynamic framework and its experimental application for investigating pKa shifting, *RNA 11*, 157-172.
6. Emilsson, G. M., Nakamura, S., Roth, A., and Breaker, R. R. (2003) Ribozyme speed limits, *RNA 9*, 907-918.